Magnetic properties, Mössbauer, and specific-heat studies of $R Ba_2Fe_3O_8$ (R = Y,Eu) compounds

I. Felner, I. Nowik, U. Yaron, O. Cohen, and E. R. Bauminger
Racah Institute of Physics, The Hebrew University, Jerusalem 91904, Israel

T. Kroener and G. Czjzek
Kernforschungszentrum Karlsruhe, Institut für Nukleare Festkörperphysik and Institut für Technische Physik, P.O.B. 3640, 76021 Karlsruhe, Germany

(Received 5 March 1993)

Complete replacement of Cu by Fe in $R Ba_2Cu_3O_7$ leads to $R Ba_2Fe_3O_8$ (R = Y and Eu). We investigated $YBa_2Fe_3O_8$ and $EuBa_2Fe_3O_8$ by several complementary experimental techniques. These compounds crystallize in a tetragonal structure with the configuration of the atoms in the unit cell very similar to that in the superconductor $YBa_2Cu_3O_7$. Magnetic-susceptibility and Mössbauer-spectroscopy measurements of ^{57}Fe and ^{151}Eu in $R Ba_2Fe_3O_8$ (R = Y and Eu) at temperatures from 4.2 to 800 K have been performed. In both compounds the iron moments order antiferromagnetically at the same Néel temperature $T_N \sim 700$ K. In $YBa_2Fe_3O_8$ the Mössbauer spectra reveal two inequivalent iron sites, probably corresponding to iron in the Fe(2) site (fivefold oxygen coordination) and in the Fe(1) site (distorted octahedral oxygen coordination). The quadrupole splitting of Fe(2) is zero. Specific-heat (C_p) measurements at different magnetic fields have been carried out between 1.5 and 30 K. The $C_p(T,H)$ curves can be resolved into a contribution of the form $C_e(T)=\gamma^* T$ with finite γ^* and a lattice contribution that consists of Debye terms. The pronounced high $\gamma^* = 10.5$ mJ/mol K^2 for $YBa_2Fe_3O_8$ is discussed.

INTRODUCTION

The study of the nonsuperconducting $R Ba_2Fe_3O_8$ (RBFO) system is very appealing, because it provides a phase having the same metal stoichiometry of superconducting $YBa_2Cu_3O_7$ (YBCO) but with copper entirely replaced by iron. Partial substitution of many kinds of metals for Cu in YBCO were carried out for the purpose of improving superconducting properties but no improvement has been found. It is well established that partial substitution of Cu in YBCO by Fe or Co, progressively decreases T_c of the system. For Fe concentration exceeding 13 at. % the materials are not superconducting.[1-3] The Fe atoms were found to occupy predominantly the Cu(1) site with an increasing fraction occupying the Cu(2) sites as the total amount of dopant increases. Full substitution by Fe^{3+} for Cu has been reported recently[4-8] and to our knowledge, no other fully substituted compounds, having the same crystal structure, have been prepared and characterized so far.

The crystal structure of the tetragonal $YBa_2Fe_3O_8$ (YBFO) was studied in detail by neutron powder diffraction.[6] The space group is $P4/mmm$, the lattice parameters and the configuration of the atoms in the unit cell are very similar to those of YBCO. The Fe(2) layers in YBFO are in a fivefold oxygen configuration similar to Cu(2) in YBCO, whereas the Fe in the Fe(1) sites, corresponding to the Cu(1) chains, are in distorted octahedral oxygen coordination forming layers, rather than the square-planar chains in YBCO. In YBFO the oxygen content is eight per formula unit,[6] thus all the possible oxygen sites in the basal plane are fully occupied.

The magnetic properties of YBFO were studied by neutron diffraction[6] and Mössbauer spectroscopy.[5] Like all the nonsuperconducting compounds which are related to YBCO,[9] YBFO exhibits an antiferromagnetically (AFM) ordering of the iron moments, but unlike YBCO the Néel temperature is high.[5] Early Mössbauer studies[5] showed that the two nonequivalent iron sites exhibit the same spectra and order at $T_N = 1020$ K. Observation of the same quadrupole interaction below and above T_N lead to the conclusion that the iron moments lie along the c axis. On the other hand, polarized neutron-diffraction measurements showed that the iron moments are perpendicular to the c axis and are coupled AFM within each Fe-O layer, as well as along the c axis.[6] Neutron-diffraction studies show[6] that the magnetic moments in the two sites are the same with an average value of 3.5 Bohr magnetons (μ_B). Electrical conductivity showed that YBFO is p type.

We present here studies of RBFO (R = Y,Eu) by several experimental techniques. Magnetic-susceptibility and ^{57}Fe Mössbauser studies reveal that both compounds are AFM ordered and both Fe sites have the same $T_N \sim 700$ K regardless of R. Our present Mössbauer studies, which are significantly different from those reported in Ref. 5, show definitely in YBFO two different subspectra for the Fe(1) and Fe(2) sites. The ^{151}Eu Mössbauer spectra of EuBFO show that Eu ions are trivalent and are exposed to an exchange field produced by the Fe sublattices. Specific-heat measurements in zero field and $H = 9$ T show no evidence of any magnetic contribution to C_p and the low γ^* values obtained for EuBFO is consistent with insulating materials. Unexpectedly, the γ^* value for YBFO is high.

0163-1829/93/48(21)/16040(7)/$06.00

SAMPLES AND EXPERIMENTAL TECHNIQUES

A. Sample preparation

The samples with the nominal composition $R\mathrm{Ba_2Fe_3O_8}$ were prepared by the solid-state reaction technique. Prescribed amounts of R_2O_3, $BaCO_3$, and Fe_2O_3 were mixed and pressed into pellets and preheated under N_2 atmosphere at 950 °C for about 1 day. The products were cooled, regrounded and fired again (under N_2 atmosphere) to 1100 °C for 48 h and then furnace cooled to ambient temperature.

B. X-ray diffraction and lattice parameters

X-ray-diffraction studies show that the compounds have a tetragonal structure with the space group $P4/mmm$. The lattice parameters for $R=$Y and Eu obtained by least-squares fits are $a=3.917$ and 3.943 Å and $c=11.825$ and 11.421 Å, respectively. The lattice parameters for YBFO and the structure parameters determined by Rietveld analysis of the full x-ray-diffraction pattern[10] are in excellent agreement with the published neutron-diffraction data.[6] The x-ray patterns indicate the presence of a few percents of the cubic $BaFeO_z$ material with $a\sim4.11$ Å, and our attempts to get completely rid of this extra phase were unsuccessful. This foreign phase is observable also in the ^{57}Fe Mössbauer spectra.

C. Mössbauer spectra

The ^{57}Fe Mössbauer spectra were measured with a 100 mCi ^{57}Co:Rh source and the ^{151}Eu spectra with a $^{151}SmF_3$ source ($\sim$200 mCi). A conventional, constant acceleration Mössbauer spectrometer was used for the present measurements. All the spectra were analyzed by least-squares fitting.

D. Magnetic measurements and calorimetry

The dc magnetic measurements on solid-ceramic pieces in the range of 5–300 K, were carried out in a commercial (Quantum Design) superconducting quantum interference device magnetometer in various applied fields. High-temperature magnetic measurements were performed over the range of 300–750 K in a 155 PAR vibrating sample magnetometer, by two different procedures. (a) The sample was at ambient temperature, a field of 500 Oe was applied, and the zero-field (ZF) magnetization was measured as a function of temperature. (b) The sample was field cooled (FC) from above T_N in the applied field, while recording the magnetization down to room temperature.

The specific heat of compact pieces (about 70 mg) cut from the pellets was measured with a semiadiabatic heat-pulse calorimeter at zero and 9 T applied fields in the temperature range of 1.5–30 K.

EXPERIMENTAL RESULTS AND DISCUSSION

A. Magnetic measurements

Our main interest here is the magnetic behavior of the two Fe sublattices. Thus, only data collected for $R=$Y and Eu will be displayed. Our ^{151}Eu Mössbauer study (to be discussed later) shows that Eu ions in EuBFO are trivalent with a nonmagnetic $J=0$ ground state. Therefore, the compound EuBFO provides an additional nonmagnetic environment for the Fe sites. The magnetic study of RBFO, where R are magnetic rare-earth elements, is now in progress and the results are planned to be published in due course.

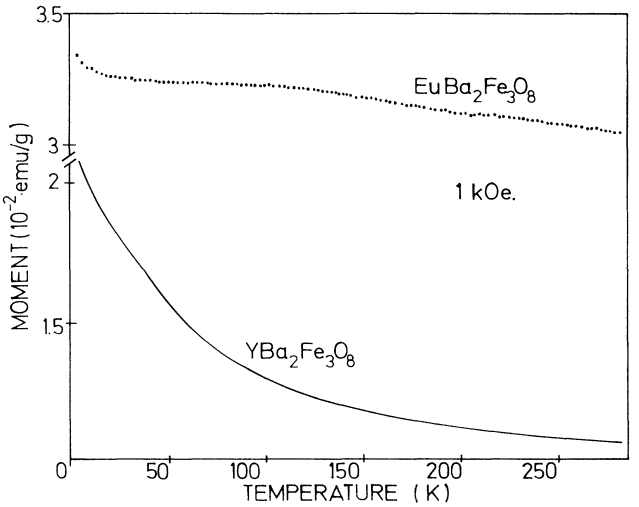

FIG. 1. Temperature dependence of the magnetic moment measured at 1 kOe for YBFO and EuBFO. (Note the plateau in the range of 20–100 K for EuBFO.)

Figures 1 and 2 exhibit the variation of the magnetization as a function of temperature for RBFO compounds. Results measured at 50 and 250 Oe and at 1 kOe show the same behavior. The small magnetization values obtained for YBFO, first decrease with increasing temperatures and then increase (Fig. 2, ZF branch) up to a maximum at $T_N=670$ K. (Note the different scales in these figures.) The shape of the magnetization curve is charac-

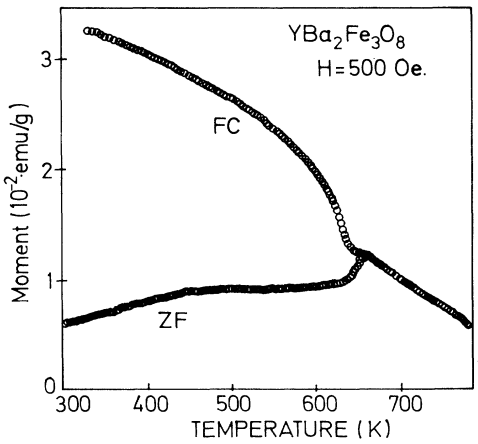

FIG. 2. Temperature dependence of the zero-field and field-cooled magnetization for YBFO at elevated temperatures measured at 500 Oe.

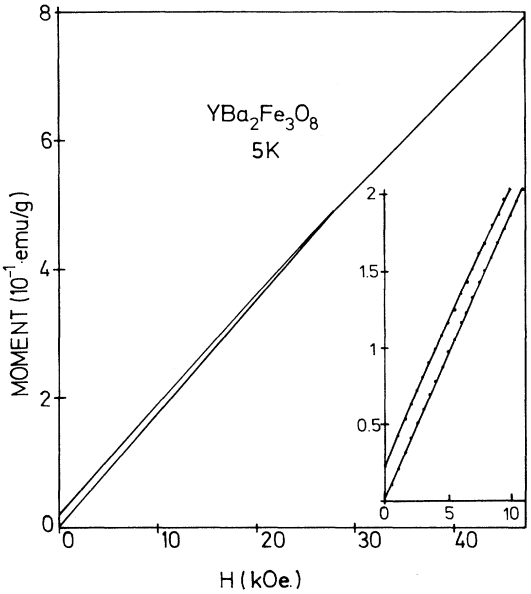

FIG. 3. Isothermal magnetization at 5 K for YBFO. Note the tiny hysteresis loop opened at 30 kOe. The parallel curves at low fields are shown in the inset.

teristic of AFM ordering of the Fe sublattices and the Néel temperature is in fair agreement with results obtained from our Mössbauer studies. For EuBFO, the higher magnetization values and the plateau in the range of 20–100 K are both due to the Van Vleck contribution of Eu^{3+} to the magnetic moments. A crude estimate of the Eu^{3+} susceptibility yields values which are in fair agreement with results for other Eu^{3+}-based compounds.[11]

The isothermal magnetization at 5 K up to 50 kOe of YBFO is shown in Fig. 3. The virgin curve is linear up to ~28 kOe where a tiny hysteresis loop is opened when the field is decreased. The inset shows the parallel curves at low fields which indicate that a constant magnetic moment (assigned as the remanent magnetization) is gained at elevated fields. The remanent magnetizations at 5K for YBFO and EuBFO are 2×10^{-2} and 9.8×10^{-3} emu/g, which correspond to 8×10^{-4} and $4.2\times10^{-4}\mu_B$/Fe, respectively. Neutron-diffraction measurements of YBFO indicate[6] an average moment of $3.5\mu_B$/Fe. This means that only a small fraction, ~0.02% for YBFO and 0.01% for EuBFO, of the Fe magnetic spins are affected by the applied field. The variation of the remanent magnetization with temperature measured at $H=0$ Oe for both materials is shown in Fig. 4. In both cases a decrease of approximately 10% is observed at the range of 5–280 K. In contrast to the results shown in Fig. 1, the remanent curve for EuBFO is well below that obtained for YBFO.

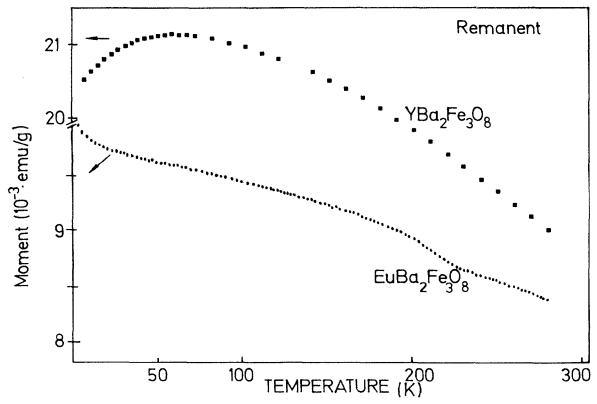

FIG. 4. Remanent magnetization as a function of temperature measured at zero field for YBFO and EuBFO.

We have also measured the FC magnetization for YBFO at high temperatures (Fig. 2). The FC magnetization increases gradually with decreasing temperature below T_N and the shape of the curve is very suggestive of a ferromagnetic alignment occurring at T_N. However, the difference between the ZF and FC branches at 350 K (2×10^{-2} emu/g) is actually (within few %) the remanent magnetization shown in Fig. 4.

The experimental results reported here (Figs. 1–4) provide an insight to the magnetic structure of the Fe sites in *R*BFO. The zero-field measurements and the linear M vs H curve at 5 K (Fig. 3), strongly support an antiferromagnetic ordering of Fe. The small magnitude of the remanent magnetization which compares well with the difference between the ZF and FC in Fig. 2, may imply that both in the FC process from above T_N and in 3 T at 5 K, the external field causes the spins to cant slightly out of their original directions. This canting produces a moment in the direction of the field and the FC curve is obtained. For EuBFO this net moment obtained is somewhat smaller than in YBFO. The temperature dependence of the remanence of both compounds (Fig. 4) indicates the freezing of the canting direction. The full knowledge of the magnetic behavior of this system can only be obtained by studying single crystals.

B. Mössbauer studies

In Fig. 5 the ^{57}Fe Mössbauer spectra of YBFO and EuBFO below and above T_N are presented. The main information obtained from visual and computer analysis is that the spectra of YBFO at 90 and 750 K are composed of two subspectra with relative intensity of 2:1. These subspectra are most probably related to Fe(2) and Fe(1) sites in the YBFO unit cell. The fit is good except in the center of the spectra where a small contribution due to the impurity $BaFeO_z$ phase is observed.[12] The detailed analysis of the YBFO spectra below T_N shows that both iron sites have the same magnetic hyperfine field (530 kOe at 4.2 K) which disappears at about 700 K (Fig. 6). The two subspectra differ only in their quadrupole interactions and the values obtained above T_N for Fe(2) and Fe(1) sites are $\Delta\equiv\frac{1}{2}eqQ\sim0$ and 1.8(1) mm/s, respectively. The effective quadrupole interactions at 90 K are $\frac{1}{2}eqQ_{\text{eff}}=0$ and -0.86 mm/s, respectively. The magnetic hyperfine field orientation relative to the tetragonal symmetry (c axis) is given by the relation

$$\tfrac{1}{2}eqQ_{\text{eff}}=\Delta(3\cos^2\Theta-1)/2\ .$$

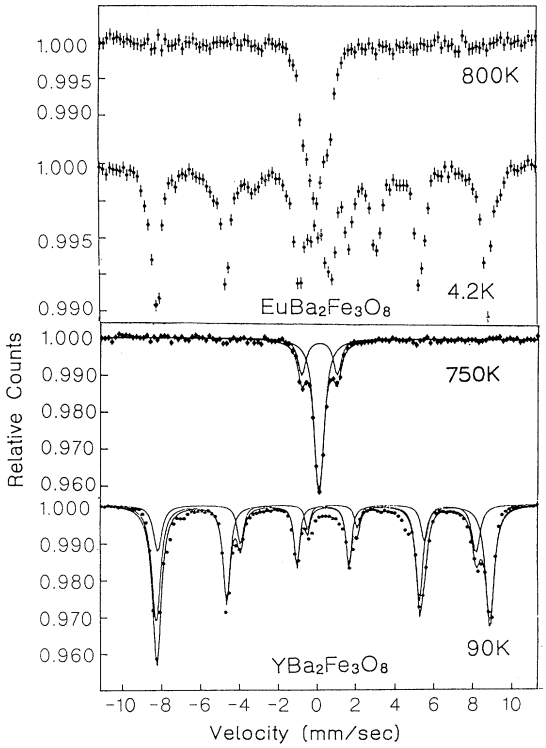

FIG. 5. Mössbauer spectra of ^{57}Fe in YBFO and EuBFO below and above T_N. The solid curves for $YBa_2Fe_3O_8$ are theoretical least-squares fit spectra.

This proves that the iron magnetic moments lie in the layers as also observed by neutron-diffraction studies.[6] Unexpectedly, this interpretation shows that $\Delta=0$ is associated with the pyramidal configuration of Fe(2), whereas the large quadrupole splitting is obtained for the distorted octahedral coordination of Fe(1) site. This Δ value is similar to that of the dominant fourfold square-planar configuration of Fe in the Cu(1) site in YBCO.[3,13]

The structural parameters of YBFO (Ref. 6) may explain the large Δ obtained for the Fe(1) site and the absence of quadrupole splitting for Fe(2). The principal difference between the structures of YBCO and YBFO arises as a consequence of the different oxygen composition which causes also different atomic positions in the two structures. Recent neutron-diffraction studies on powder YBCO material[14] determine the atomic positions of Cu(2) and the apical O(1) as (0,0,0.3554) and (0,0,0.1595), respectively, and the lattice parameter $c=11.633$ Å. Thus the Cu(2)-O(1) distance 2.278 Å is 22% *longer* than the Cu(1)-O(1) distance—1.855 Å. On the other hand, the atomic positions in YBFO (Fig. 7) for

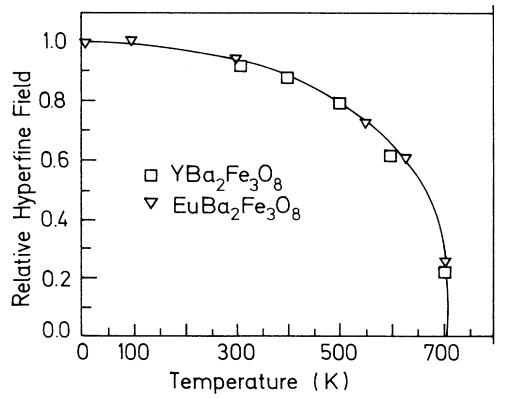

FIG 6. Temperature dependence of the average hyperfine field acting on iron nuclei in $YBa_2Fe_3O_8$ and $EuBa_2Fe_3O_8$.

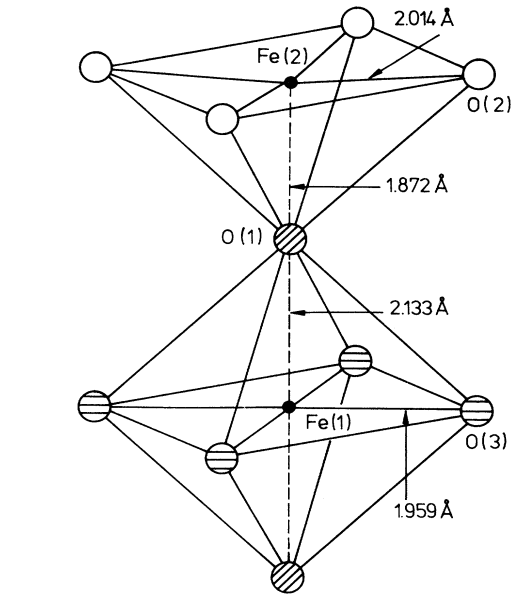

FIG. 7. Coordination of oxygen and distances around Fe(1) and Fe(2) in the YBFO structure.

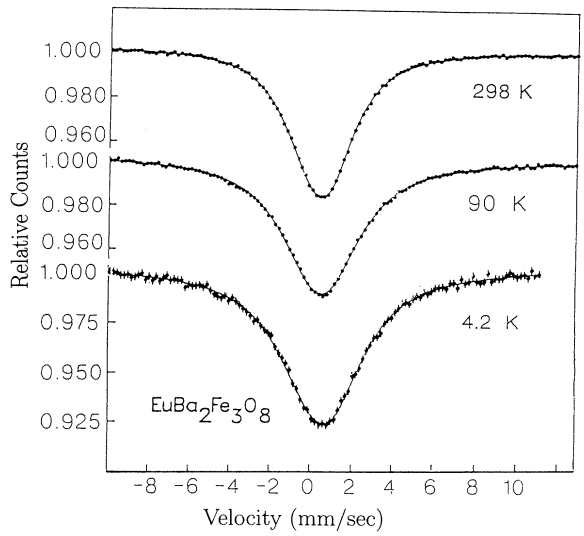

FIG. 8. Mössbauer spectra of ^{151}Eu in $EuBa_2Fe_3O_8$ at several temperatures. The solid curves are theoretical least-squares fit spectra.

Fe(2) and O(1) are (0,0,0.3388) and (0,0,0.1804) Å, respectively. Assuming $a=3.917$ Å and $c=11.825$ Å, we obtain that the Fe(2)-O distances in the pyramid range from 1.872 Å for the apical distance to 2.014 Å for the in-plane separation. The coordination polyhedra of Fe(1) are distorted octahedra with 1.959 Å for the Fe(1)-O(3) distance in the basal plane and 2.133 Å for Fe(1)-O(1). Thus the Fe(2)-O(1) distance is 14% *shorter* than the Fe(1)-O(1) separation. It appears that in YBFO the apical O(1) atom moves away from its original position in YBCO toward the Fe(2) layers by ~0.4 Å. In this position the distance of Fe(2) to all its five oxygen neighbors is more equal, and the quadrupole-splitting value, which is extremely sensitive to the Fe(2)-O(1) distance,[15] is practically zero. The large Fe(1)-O(1) distance is also responsible for the rise of the quadrupole splitting of the Fe(1) site, in which the local environment of Fe is square planar rather than octahedral. First-nearest-neighbor point-charge calculations of the electric-field gradients for the two sites in YBFO confirm this interpretation. Generally speaking, we obtain that the quadrupole splitting for the distorted octahedral Fe(1) site, is three times larger than that of the pyramidal Fe(2) site.

The Mössbauer spectra of EuBFO are qualitatively similar to those of YBFO (Fig. 5), yet the two Fe sites are indistinguishable. Smeared single-site Mössbauer spectra with broadened absorption lines were observed. The magnetic hyperfine splitting disappears also at ~700 K (Fig. 6) proving that both YBFO and EuBFO have the same T_N. It should be mentioned that results similar to EuBFO were also obtained for $HoBa_2Fe_3O_8$ and $ErBa_2Fe_3O_8$.[8]

The fact that we observe for YBFO the Fe(2) and Fe(1) sites separately, whereas in EuBFO one can hardly identify two sites, and only one single iron spectrum was observed in Ref. 5, needs some consideration. It seems to us that the distinction between the two sites depends on the exact concentration of oxygen. If the oxygen concentration is very close to eight, the iron nuclei in the two iron sites experience different quadrupole interactions and two Mössbauer subspectra are observed. For lower oxygen content, the Fe(1) site misses oxygen as first-nearest neighbors, the quadrupole interactions have a distribution in values and only smeared spectra are obtained.

The ^{151}Eu Mössbauer spectra of EuBFO shown in Fig. 8 were fitted by a theoretical spectrum with isomer shift, quadrupole interaction and a distribution of hyperfine fields, as free parameters. The surprising discovery was that the average hyperfine field was 22 kOe at 4.2 K and not zero. The quadrupole interaction is 1.45 mm/s at 4.2 K and changes little with temperature. The isomer shift is 0.5 mm/s at 4.2 K. These results show that the Eu ion is trivalent and that it is exposed to a magnetic exchange field.[16] Since the rare earth is located in a position surrounded by eight antiferromagnetically ordered Fe(2) ions in a perfectly symmetric arrangement, it is surprising to find that nonzero exchange field is acting on the Eu ion. However, if the oxygen concentration is less than eight, the contribution to the exchange field from farther Fe(1) neighbors will not cancel out and a distribution of exchange fields will act on the Eu ions, as observed experimentally.

C. Specific-heat measurements

Because of the similarity between the crystal structures of RBFO and YBCO and the question whether or not the linear specific-heat coefficient γ in YBCO is an intrinsic property, we also measured the specific heat C_p of RBFO at low temperatures. Figures 9 and 10 exhibit the curves of C_p against T for EuBFO and YBFO at $H=0$ and $H=9$ T in double-log plots. The small values of the specific heat suggest contributions mainly from lattice vibrations and the full $C_p(T)$ curves in the temperature range between 1.5–15 K were therefore fitted with the sum of a Debye-model approximation $[C_L(T)=\beta T^3-\delta T^5]$ for the lattice contribution to determine the Debye temperature θ_D and a linear term for the nonzero remanent electronic contribution $C_e(T)=\gamma^* T$: $C_p(T)=C_e(T)+C_L(T)$.

No specific-heat feature indicative of magnetic origin can be observed in the $C_p(T)$ data for EuBFO (Fig. 10) which, along with the magnetic measurements and

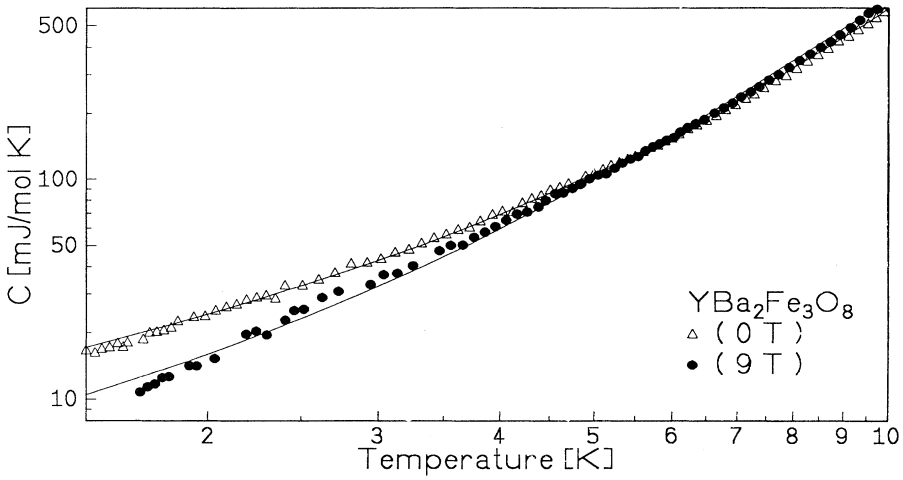

FIG. 9. Specific heat C_p of YBFO as a function of temperature for external fields $H=0$ and $H=9$ T. The solid lines are the least-squares fit of the total $C_p(T)$.

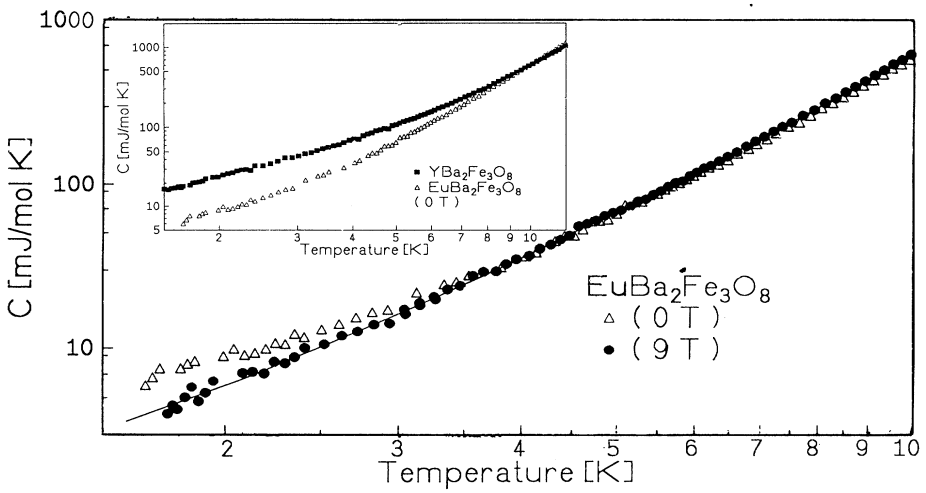

FIG. 10. Specific heat C_p of YBFO as a function of temperature for external fields $H=0$ and $H=9$ T. The solid line is the least-squares fit of $C_p(T)$. The inset shows $C_p(T)$ at $H=0$ T for YBFO and EuBFO.

Mössbauer studies described above, is consistent with the Eu^{3+} $J=0$ nonmagnetic ground state. In contrast, for $ErBa_2Fe_3O_8$ (not shown here) as small upturn is observed at low temperatures. This anomaly can be regarded as a hint for AFM order of the Er sublattice at a temperature lower than 1.5 K.

The specific heat above 5 K is dominated by the field independent C_L and the fit of C_p data for $T \leq 15$ K yields the values for the coefficients $\beta=0.464$ and 0.416 mJ/mol K^4, corresponding to Debye temperatures $\theta_D=390(5)$ and 430(5) K for EuBFO and YBFO, respectively. These values are in perfect agreement with the average Θ_D suggested for YBCO, (410±35 K).[17] The typical spin-wave contribution to C_p for an AFM material $C_M \propto T^3$, is assumed to be very small in accordance with the large value of T_N and cannot be extracted from our data.

The excess contribution to C_p below 5 K is sample and field dependent. The linear coefficients γ^* for $C_e(T)$ obtained are 2.5(1) and 1.1(1) mJ/mol K^2 for EuBFO and 10.5(3) and 5.7(2) mJ/mol K^2 for YBFO for $H=0$ and 9 T, respectively.

For EuBFO at $H=0$ the linear γT term for C_e is not explicit, and an attempt to use a power law for C_e: $C_e=\gamma^* T^\alpha$, where α is a free parameter yields $\gamma^*=4.0(2)$ mJ/mol K and $\alpha=0.4$ but did not improve the fit. The small γ^* values obtained for EuBFO are not surprising and are consistent with the expectation for an insulating solid. These values agree well with the estimated finite value of $\gamma=1.4$ mJ/mol K for YBCO (Refs. 17 and 18) in both superconducting and antiferromagnetic states, proving that $BaFeO_z$, which exists as an extra phase in EuBFO, does not contribute to γ^*. The effect of an applied magnetic field on C_e at low temperatures is described in detail by Schreiner *et al.*,[19] and our present results (Figs. 9 and 10) are consistent with the $C_p(T,H)$ data published for YBCO.[19] Figure 10 (inset) shows the $C_p(T)$ at $H=0$ T for YBFO and EuBFO, and the discrepancy between the two curves is clearly observed. The high C_p values for YBFO at $T<8$ K are due to the remarkably high γ^* (10.5 mJ/mol K^2).

The origin for this high γ^* is unclear. It is not a result of a different contribution of the magnetic term C_M to C_p, because both materials have the same T_N (Fig. 6) and magnetic hyperfine fields at 4.2 K (Fig. 5). The difference between YBFO and EuBFO described now as well as the different Mössbauer spectra obtained, may result from different stoichiometry of oxygen in these materials. This explanation is clearly in conflict with data obtained in YBCO, where γ is not affected much by oxygen depletion.[17] Moreover, it was shown[19] that the size of γ^* in YBCO, is strongly influenced by disorder induced to the material whether by irradiation with fast neutrons, or by substitution with other elements for Cu. Thus it was assumed that an intrinsic disorder in YBCO is the preferable origin for γ^*. But, such an explanation has to be reconciled with our Mössbauer studies (Fig. 5), which clearly indicate that (at least) the oxygen configuration around the Fe sublattices is more ordered in YBFO than in EuBFO. Thus, the intriguing question remains, as to why γ^* is high in YBFO material.

CONCLUSIONS

We have reported the magnetic properties and specific heats of $RBa_2Fe_3O_8$ (R = Y and Eu) which have the same metal stoichiometry as YBCO but with copper entirely replaced by iron. Magnetic susceptibilities and ^{57}Fe Mössbauer studies show that the both Fe sites are AFM ordered with the same $T_N \sim 700$ K regardless of R. The Mössbauer studies on YBFO show two different subspectra for Fe(1) and Fe(2) sites and the zero quadrupole splitting of the pyramidal configuration of Fe(2) is caused by the short Fe(2)-O(1) distance. This atomic position leads to a large quadrupole splitting in the octahedral Fe(1) site. Specific-heat measurements show that the coefficient of the linear term γ^* is low in EuBFO (as expected) but significantly high in YBFO. The origin for this high γ^* value is not yet explained.

ACKNOWLEDGMENTS

The authors are very grateful to Dr. The. Schreiner for very fruitful discussions and for his assistance with the specific-heat data. One of us (I.F.) is indebted to Kernforschungszentrum Karlsruhe (INFP) for hospitality in the last stage of this research. The research was supported by Israeli Ministry of Science and Technology and by the Clazky Foundation for Superconductivity.

[1]P. H. Hor *et al.*, Phys. Rev. Lett. **58**, 1891 (1987).
[2]I. Felner, I. Nowik, and Y. Yeshurun, Phys. Rev. B **36**, 3823 (1987).
[3]D. Hechel *et al.*, Phys. Rev. B **42**, 2166 (1990).
[4]Y. Matsumoto and J. Hombo, J. Solid State Chem. **93**, 395 (1991).
[5]M. El Massalami *et al.*, Physica C **183**, 143 (1991).
[6]Q. Huang *et al.*, Phys. Rev. B **45**, 9611 (1992).
[7]P. Karen, P. H. Andersen, and A. Kjekshus, J. Solid State Chem. **101**, 48 (1992).
[8]O. Cohen, I. Felner, I. Nowik, U. Yaron, and E. R. Bauminger, Hyperfine Interact. (to be published).
[9]I. Felner *et al.*, Phys. Rev. Lett. **65**, 1945 (1990).
[10]G. Roth (private communication).
[11]E. Bucher *et al.*, Phys. Rev. B **11**, 440 (1975); W. E. Gardner, J. Penfold, and I. R. Harris, J. Phys. C **1**, 1139 (1971).
[12]I. Ichida *et al.*, Bull. Inst. Chem. Res. **51**, 295 (1973).
[13]I. S. Lyubutin *et al.*, Physica C **195**, 383 (1992).
[14]M. Guillaume *et al.*, Z. Phys. B **90**, 13 (1993).
[15]A. Rykov *et al.*, Physica C **205**, 63 (1993).
[16]I. Nowik and S. Ofer, Phys. Rev. **153**, 409 (1967).
[17]A. Junod, in *Physical Properties of High-T_c Superconductors II,* edited by D. M. Ginsberg (World Scientific, Singapore, 1990), p. 13.
[18]S. J. Collocott, R. Driver, and E. R. Vance, Phys. Rev. B **41**, 6329 (1990).
[19]Th. Schreiner *et al.*, Physica C **204**, 161 (1992).